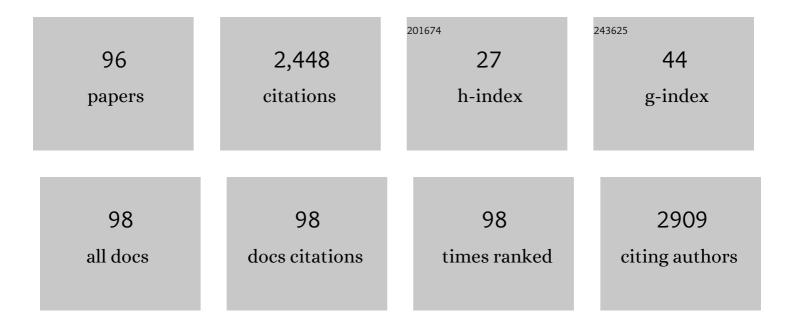
List of Publications by Year in descending order

Source: https://exaly.com/author-pdf/4713895/publications.pdf Version: 2024-02-01



Διι Νεματι

#	Article	IF	CITATIONS
1	The relation between particle size and transformation temperature of gibbsite to <i>α</i> LPHA-alumina. Mineral Processing and Extractive Metallurgy: Transactions of the Institute of Mining and Metallurgy, 2022, 131, 111-121.	0.2	1
2	Investigation of interfacial and mechanical properties of alumina-coated steel fiber reinforced geopolymer composites. Construction and Building Materials, 2021, 288, 123118.	7.2	28
3	The effect of mixing molar ratios and sand particles on microstructure and mechanical properties of metakaolin-based geopolymers. Materials Chemistry and Physics, 2020, 240, 122223.	4.0	32
4	Comparison between electrochemical and photoelectrochemical detection of dopamine based on titania-ceria-graphene quantum dots nanocomposite. Biosensors and Bioelectronics, 2020, 151, 111977.	10.1	58
5	Effect of YSZ sol-gel coating on interaction of Crofer22 APU with sealing glass for solid oxide fuel/electrolysis cell. Journal of Alloys and Compounds, 2020, 847, 156496.	5.5	10
6	Synthesis and characterization of rGO/Fe2O3 nanocomposite as an efficient supercapacitor electrode material. Journal of Materials Science: Materials in Electronics, 2020, 31, 14998-15005.	2.2	15
7	Hydrophobic octadecylamine-functionalized graphene/TiO2 hybrid coating for corrosion protection of copper bipolar plates in simulated proton exchange membrane fuel cell environment. International Journal of Hydrogen Energy, 2020, 45, 15380-15389.	7.1	46
8	Magnetic CoFe2O4 nanoparticles doped with metal ions: A review. Ceramics International, 2020, 46, 18391-18412.	4.8	155
9	Grain growth kinetics and electrical properties of CuO doped SnO2-based varistors. Journal of Alloys and Compounds, 2019, 770, 784-791.	5.5	14
10	SiC fines effects on the microstructure and properties of bauxite-based low-cement refractory castables. Ceramics International, 2019, 45, 16338-16346.	4.8	3
11	Gel combustion synthesis of fluorine-doped tin oxide and its characteristics: applying D-optimal factorial design of experiment. Bulletin of Materials Science, 2019, 42, 1.	1.7	1
12	Pressureless sintering of ZrB2 ceramics codoped with TiC and graphite. International Journal of Refractory Metals and Hard Materials, 2019, 81, 189-195.	3.8	68
13	Photocatalytic and photoluminescence properties of ZnO/graphene quasi core-shell nanoparticles. Ceramics International, 2019, 45, 8945-8961.	4.8	21
14	Dispute in photocatalytic and photoluminescence behavior in ZnO/graphene oxide core-shell nanoparticles. Materials Letters, 2019, 240, 117-120.	2.6	6
15	Phase and microstructural evolution of low carbon MgO-C refractories with addition of Fe-catalyzed phenolic resin. Ceramics International, 2019, 45, 3390-3406.	4.8	38
16	The role of oxygen defects in magnetic properties of gamma-irradiated reduced graphene oxide. Journal of Alloys and Compounds, 2019, 784, 134-148.	5.5	22
17	Microstructural, optical, and electrical characteristics of Ni/C doped BST thin films. Ceramics International, 2019, 45, 5503-5510.	4.8	11
18	Hydrothermal synthesis of TiO2 nanorod for using as an electron transport material in perovskite solar cells. AIP Conference Proceedings, 2018, , .	0.4	10

#	Article	IF	CITATIONS
19	Conventional and two step sintering of PZT-PCN ceramics. Applied Physics A: Materials Science and Processing, 2018, 124, 1.	2.3	6
20	Synthesis and properties of Ce-doped TiO2-reduced graphene oxide nanocomposite. Journal of Alloys and Compounds, 2018, 742, 986-995.	5.5	35
21	Catalytic graphitization behavior of phenolic resins by addition of in situ formed nano-Fe particles. Physica E: Low-Dimensional Systems and Nanostructures, 2018, 101, 50-61.	2.7	32
22	Recent Advancements in Bulk Metallic Glasses and Their Applications: A Review. Critical Reviews in Solid State and Materials Sciences, 2018, 43, 233-268.	12.3	170
23	Doxorubicin-conjugated D-glucosamine- and folate- bi-functionalised InP/ZnS quantum dots for cancer cells imaging and therapy. Journal of Drug Targeting, 2018, 26, 267-277.	4.4	51
24	Reduced graphene oxide: An alternative for Magnetic Resonance Imaging contrast agent. Materials Letters, 2018, 233, 363-366.	2.6	9
25	Magnetron-sputtered TixNy thin films applied on titanium-based alloys for biomedical applications: Composition-microstructure-property relationships. Surface and Coatings Technology, 2018, 349, 251-259.	4.8	56
26	A comparative evaluation of the additional impact of nanometer-sized tetravalent oxides on the performance of Doloma-Magnesia ceramic refractories. Ceramics International, 2018, 44, 2058-2064.	4.8	12
27	Interactions near the triple-phase boundaries metal/glass/air in planar solid oxide fuel cells. International Journal of Hydrogen Energy, 2017, 42, 5306-5314.	7.1	13
28	Microwave-assisted sintering of Al 2 O 3 -MWCNT nanocomposites. Ceramics International, 2017, 43, 6105-6109.	4.8	13
29	Influence of synthesis variables on the properties of barium hexaferrite nanoparticles. Journal of Materials Science: Materials in Electronics, 2017, 28, 4606-4612.	2.2	5
30	Performance improvement of MgO-CaO refractories by the addition of nano-sized Al 2 O 3. Materials Chemistry and Physics, 2017, 198, 354-359.	4.0	40
31	Fabrication of SiC body by microwave sintering process. Journal of Materials Science: Materials in Electronics, 2017, 28, 5675-5685.	2.2	4
32	Effects of Fe2O3 content on ionic conductivity of Li2O-TiO2-P2O5 glasses and glass-ceramics. Materials Chemistry and Physics, 2017, 190, 8-16.	4.0	15
33	Preparation, magnetic properties, and photocatalytic performance under natural daylight irradiation of Fe 3 O 4 -ZnO core/shell nanoparticles designed on reduced GO platelet. Materials Science in Semiconductor Processing, 2017, 72, 85-92.	4.0	33
34	The Effect of Fatty Amine Chain Length on Synthesis Process of Inp/Zns Quantum Dots. Oriental Journal of Chemistry, 2016, 32, 2163-2169.	0.3	8
35	Effect of Samarium Oxide on the Electrical Conductivity of Plasma-Sprayed SOFC Anodes. Jom, 2016, 68, 2569-2573.	1.9	6
36	Molten salt synthesis of a SiC coating on graphite flakes for application in refractory castables. Ceramics International, 2016, 42, 11951-11957.	4.8	35

#	Article	IF	CITATIONS
37	Densification and Properties of Fe2O3 Nanoparticles added CaO Refractories. Ceramics International, 2016, 42, 12270-12275.	4.8	42
38	New Bi-Gravity from New Massive Gravity. Journal of High Energy Physics, 2016, 2016, 1.	4.7	4
39	Microwave absorption properties of Ti–Zn substituted strontium hexaferrite. Journal of Materials Science: Materials in Electronics, 2016, 27, 1901-1905.	2.2	7
40	Cold compaction behavior and pressureless sinterability of ball milled WC and WC/Cu powders. Science of Sintering, 2016, 48, 71-79.	1.4	4
41	Corrosion protection of 1050 aluminium alloy using a smart self-cleaning TiO2–CNT coating. Surface and Coatings Technology, 2015, 275, 224-231.	4.8	15
42	Synthesis of C–N–Y tri-doped TiO ₂ photo-catalyst for MO degradation and characterization. Materials Research Express, 2015, 2, 105011.	1.6	6
43	Effects of Ce–Co substitution on structural, magnetic and dielectric properties of M-type barium hexaferrite nanoparticles synthetized by sol–gel auto-combustion route. Journal of Materials Science: Materials in Electronics, 2015, 26, 2134-2144.	2.2	39
44	Comprehensive study on the effect of SiC and carbon additives on the pressureless sintering and microstructural and mechanical characteristics of new ultra-high temperature ZrB2 ceramics. Ceramics International, 2015, 41, 11456-11463.	4.8	30
45	Dielectric and piezoelectric properties of porous PZT–PCN ceramics sintered at different temperatures. Materials Letters, 2015, 151, 85-88.	2.6	18
46	Effects of processing conditions on the physico-chemical characteristics of titanium dioxide ultra-thin films deposited by DC magnetron sputtering. Ceramics International, 2015, 41, 7977-7981.	4.8	10
47	Effect of intermediate nickel layer on seal strength and chemical compatibility of glass and ferritic stainless steel in oxidizing environment for solid oxide fuel cells. International Journal of Hydrogen Energy, 2015, 40, 16434-16442.	7.1	13
48	Effect of working pressure and annealing temperature on microstructure and surface chemical composition of barium strontium titanate films grown by pulsed laser deposition. Bulletin of Materials Science, 2015, 38, 1645-1650.	1.7	30
49	Influence of Fe 2 O 3 on non-isothermal crystallization kinetics and microstructure of lithium titanium phosphate glass-ceramics. Journal of Non-Crystalline Solids, 2015, 408, 130-136.	3.1	17
50	One-pot synthesis of ZnO nanoparticles and submicron-aggregates for dye-sensitized solar cells. Materials Letters, 2015, 139, 433-436.	2.6	5
51	Nanothickness films, nanostructured films, and nanocrystals of barium titanate obtained directly by a newly developed sol–gel synthesis pathway. Journal of Materials Science: Materials in Electronics, 2014, 25, 5345-5355.	2.2	23
52	Effect of Ti–Zn substitution on structural, magnetic and microwave absorption characteristics of strontium hexaferrite. Journal of Alloys and Compounds, 2014, 583, 325-328.	5.5	96
53	Evaluation of ascorbic acid-loaded calcium phosphate bone cements: Physical properties and in vitro release behavior. Ceramics International, 2014, 40, 3961-3968.	4.8	19
54	Synthesis and characterization of co-doped TiO2 thin films on glass-ceramic. Materials Science in Semiconductor Processing, 2014, 26, 41-48.	4.0	15

#	Article	IF	CITATIONS
55	Enhancing glass ionomer cement features by using the HA/YSZ nanocomposite: A feed forward neural network modelling. Journal of the Mechanical Behavior of Biomedical Materials, 2014, 29, 317-327.	3.1	25
56	Crack-free nanostructured BaTiO3 thin films prepared by sol–gel dip-coating technique. Ceramics International, 2014, 40, 8613-8619.	4.8	61
57	Improving CNT distribution and mechanical properties of MWCNT reinforced alumina matrix. Materials Science & Engineering A: Structural Materials: Properties, Microstructure and Processing, 2014, 617, 110-114.	5.6	22
58	Optimization of the magnetic properties and microstructure of Co2+–La3+ substituted strontium hexaferrite by varying the production parameters. Ceramics International, 2014, 40, 5675-5680.	4.8	16
59	Effect of simultaneous chemical substitution of A and B sites on the electronic structure of BiFeO3 films grown on BaTiO3/SiO2/Si substrate. Journal of Materials Science: Materials in Electronics, 2013, 24, 2128-2134.	2.2	26
60	The effect of functionalisation method on the stability and the thermal conductivity of nanofluid hybrids of carbon nanotubes/gamma alumina. Ceramics International, 2013, 39, 3885-3891.	4.8	168
61	Synthesis of nanocrystalline Ni/Ce-YSZ powder via a polymerization route. Materials Science-Poland, 2013, 31, 343-349.	1.0	0
62	Effect of chemical substitution on the morphology and optical properties of Bi1â^'xCaxFeO3 films grown by pulsed-laser deposition. Journal of Materials Science: Materials in Electronics, 2013, 24, 248-252.	2.2	23
63	Synthesis and characterisation of $\langle i \rangle \hat{l}^2 \langle i \rangle$ -tricalcium phosphate coating on zirconia toughened alumina by biomimetic method. Advances in Applied Ceramics, 2013, 112, 140-145.	1.1	2
64	EFFECT OF MgO NANO PARTICLES ON SINTERING BEHAVIOR OF Al2O3-SiC-MgO NANO COMPOSITES. International Journal of Modern Physics Conference Series, 2012, 05, 568-573.	0.7	2
65	Synthesis and crystallization of lead–zirconium–titanate (PZT) nanotubes at the low temperature using carbon nanotubes (CNTs) as sacrificial templates. Advanced Powder Technology, 2012, 23, 647-654.	4.1	9
66	Influence of NaF on Crystallization and Machinability of Mica Glass Ceramics. Synthesis and Reactivity in Inorganic, Metal Organic, and Nano Metal Chemistry, 2012, 42, 958-964.	0.6	3
67	Role of MgF2 on properties of glass–ceramics. Bulletin of Materials Science, 2012, 35, 853-858.	1.7	9
68	Protection of titanium metal by nanohydroxyapatite coating with zirconia and alumina second phases. Protection of Metals and Physical Chemistry of Surfaces, 2012, 48, 688-691.	1.1	0
69	Effect of different additives on the properties of alumina-spinel castables. Ceramica, 2012, 58, 489-494.	0.8	1
70	Microwave assisted synthesis & properties of nano HA-TCP biphasic calcium phosphate. International Journal of Minerals, Metallurgy and Materials, 2012, 19, 441-445.	4.9	18
71	Preparation and characterisation of diopside-based glass–ceramic foams. Ceramics International, 2012, 38, 2005-2010.	4.8	50
72	The effects of SiO2 and K2O on glass forming ability and structure of CaO TiO2P2O5 glass system. Ceramics International, 2012, 38, 3281-3290.	4.8	12

#	Article	IF	CITATIONS
73	Microstructural features of nanocomposite of alumina@carbon nanotubes/alumina nanoparticles synthesized by a solvothermal method. Ceramics International, 2012, 38, 3991-3998.	4.8	8
74	Electronic structure and morphological study of BaTiO3 film grown by pulsed-laser deposition. Materials Letters, 2012, 72, 107-109.	2.6	24
75	Conductor–insulator transition and electronic structure of Ca-doped BiFeO3 films. Materials Letters, 2012, 83, 124-126.	2.6	27
76	Synthesis and characterization of hydroxyapatite/titania nanocomposites using in situ precipitation technique. Superlattices and Microstructures, 2012, 51, 877-885.	3.1	29
77	Effects of nucleation agents on the preparation of transparent glass–ceramics. Journal of the European Ceramic Society, 2012, 32, 2989-2994.	5.7	24
78	Characterization and photocatalytic activities of nanosized titanium dioxide thin films. International Journal of Environmental Science and Technology, 2011, 8, 545-552.	3.5	11
79	Adsorption of hydrocarbons on modified nanoclays. IOP Conference Series: Materials Science and Engineering, 2011, 18, 182012.	0.6	7
80	A modified method for barium titanate nanoparticles synthesis. Materials Research Bulletin, 2011, 46, 2291-2295.	5.2	59
81	Investigation of dark and light conductivities in calcium doped bismuth ferrite thin films. Materials Letters, 2011, 65, 3086-3088.	2.6	17
82	Effect of Y2O3 and Er2O3 co-dopants on phase stabilization of bismuth oxide. Ceramics International, 2011, 37, 3451-3455.	4.8	39
83	Photoconductivity and diode effect in Bi rich multiferroic BiFeO3 thin films grown by pulsed-laser deposition. Journal of Materials Science: Materials in Electronics, 2011, 22, 815-820.	2.2	23
84	Sintering of Al2O3–SiC composite from sol–gel method with MgO, TiO2 and Y2O3 addition. Ceramics International, 2011, 37, 1681-1688.	4.8	17
85	Two-step sintering of ZnO varistors. Solid State Ionics, 2011, 190, 99-105.	2.7	34
86	Synthesis and Characterization of Al ₂ O ₃ -SiC Nano Composite by Sol-Gel Method and the Effect of TiO ₂ on Sintering. Journal of Nano Research, 2011, 13, 7-19.	0.8	4
87	Effect of Iron Oxide and Silica Doping on Microstructure, Bandgap and Photocatalytic Properties of Titania by Water-in-Oil Microemulsion Technique. Transactions of the Indian Ceramic Society, 2011, 70, 227-232.	1.0	4
88	Utilization of DTA in the Determination of a Crystallization Mechanism in Transparent Glass-Ceramics with a Nanocrystalline Structure. Synthesis and Reactivity in Inorganic, Metal Organic, and Nano Metal Chemistry, 2011, 41, 561-570.	0.6	7
89	High voltage SnO2 varistors prepared from nanocrystalline powders. Journal of Materials Science: Materials in Electronics, 2010, 21, 199-205.	2.2	5
90	Microstructural and electrical properties of varistors prepared from coated ZnO nanopowders. Journal of Materials Science: Materials in Electronics, 2010, 21, 571-577.	2.2	19

#	Article	IF	CITATIONS
91	Crystallisation kinetics of hydroxyapatite thin films prepared by sol-gel process. Advances in Applied Ceramics, 2010, 109, 313-317.	1.1	7
92	Effects of nucleation agent particle size on properties, crystallisation and microstructure of glass-ceramics in TiO ₂ -ZrO ₂ -Li ₂ O-CaO- Al ₂ O ₃ -SiO ₂ system. Advances in Applied Ceramics, 2010, 109, 318-323.	1.1	10
93	Properties, crystallization mechanism and microstructure of lithium disilicate glass–ceramic. Journal of Non-Crystalline Solids, 2010, 356, 208-214.	3.1	65
94	Characterization of optical properties of amorphous BaTiO3 nanothin films. Journal of Non-Crystalline Solids, 2009, 355, 2480-2484.	3.1	62
95	Production of perovskite catalysts on ceramic monoliths with nanoparticles for dual fuel system automobiles. International Journal of Environmental Science and Technology, 2009, 6, 105-112.	3.5	18
96	The Effects of Composition and Sintering Conditions on Zirconia Toughened Alumina (ZTA) Nanocomposites. Advanced Materials Research, 0, 93-94, 695-698.	0.3	5